Brillouin scattering from shear horizontal surface phonons in silicon on insulator structures: Theory and experiment

G. Ghislotti and C. E. Bottani*
Dipartimento di Ingegneria Nucleare del Politecnico di Milano, Via Ponzio, 34/3-20133 Milano, Italy
(Received 12 May 1994)

We used Brillouin scattering in *p-s* polarization to study shear horizontal (SH) acoustic surface phonons in a silicon-on-insulator structure made of a Si/SiO_2 bilayer on a Si substrate. Two main peaks were measured, the first belonging to the discrete part and the second to the continuous part of the spectrum. The latter feature originates from a type of pseudosurface wave, or quasiresonance, typical of the investigated structure [Bottani *et al.*, J. Phys. Condens. Matter **6**, L85 (1994)]. Because of the SH polarization of the phonons considered Brillouin scattering takes place only via the elasto-optic mechanism, that is, by modulation of the bulk dielectric function of the material. To fully explain the experimental data we performed a computation of the *p-s* Brillouin cross section. The SH phonon spectrum, both discrete and continuous, was computed numerically using a slab approximation. The guided-wave nature of the discrete mode and the strong surface localization of the pseudomode are illustrated by means of the layer projected phonon density of states. We computed the incident *p* electric field transmitted in the medium and the fluctuating polarization vector radiating Brillouin light. The *p-s* cross section was evaluated using a Green-function method introduced some time ago by Laks and Mills [Phys. Rev. B **20**, 4962 (1979)] The computed intensity of the scattered field is in good agreement with the experimental finding.

I. INTRODUCTION

The spectrum of long-wavelength surface acoustic phonons in opaque or semiopaque materials has been extensively investigated by means of Brillouin light scattering. Most of the studies have dealt with surface acoustic phonons polarized in the sagittal plane, defined by the surface phonon propagation wave vector $\mathbf{q}_{||}$ and the surface normal. For this type of excitation, light scattering occurs through the surface ripple and volume elasto-optic effects and the Brillouin scattering cross section, which depends on both these mechanisms, can show strong interference features.[1] So far the case of shear horizontal (SH) phonons, that is, transverse phonons polarized in the plane of the surface, has received little attention at least from the experimental point of view. Although a great deal of acoustic and geophysical literature exists about shear horizontal surface elastic waves[2] and although the corresponding mathematical treatment is easier than that needed to treat sagittal waves, SH thermal waves (phonons) have been considered as sources of surface Brillouin scattering in a very limited number of papers and only in the case of supported films.

Since SH waves are polarized parallel to the surface, the mechanism of their interaction with the light is only the volume elasto-optic effect and no interference phenomena coming from scattering off the thermal surface ripple (as in the case of sagittal modes) can appear in the spectrum. Calculations of the Brillouin scattering cross section for SH surface acoustic modes (in the discrete part of the spectrum these modes are called Love modes) have been performed by Bortolani *et al.*,[3] by Albuquerque *et al.*,[4] and by Mayer[5], who performed a full quantum-mechanical computation of the cross section for a dielectric layered film on a metallic substrate, but at that time these authors could not compare their theoretical predictions with any experimental data.

To our knowledge there are up to now only two reported experimental works on the detection of SH surface acoustic phonons using Brillouin scattering. The first was conducted by Bell *et al.*[6] in Nb/Cu superlattice on a sapphire substrate. Those authors performed their measurements by detecting the tails of the acoustic modes in the sapphire substrate and gave no evidence of SH acoustic modes in the continuum part of the spectrum.

The second, by Bottani *et al.*,[7] announced the observation of SH surface acoustic modes in both the discrete and continuum parts of the spectrum in the same silicon-on-insulator structure that we are concerned with in the present paper. In that paper the theory was limited to the acoustic part and the Brillouin cross section was not evaluated. In the present paper we investigate surface *p-s* Brillouin scattering in a silicon on insulator (SOI) structure composed of a silicon dioxide layer buried in a Si(001) substrate. The structure was produced by oxygen implantation and subsequent high temperature treatment of a Si(001) wafer (SIMOX technology: separation by implantation of oxygen).

The thickness of the buried oxide L and of the top silicon layer d was measured by cross-sectional transmission electron microscopy to be respectively 110 nm and 350 nm as in Ref. 7. Observations were conducted for phonons propagating along ⟨100⟩. Experiments and theory concerning *p-p* Brillouin scattering from sagittal modes in similar systems are presented elsewhere by Nizzoli *et al.*[8] The present paper is organized as follows:

 ©1994 The American Physical Society

(i) We discuss the spectrum of surface SH phonons in the structure presenting the layer projected phonon density of states (LPPDS) for the SH polarization. This spectral density was derived from the corresponding Green function which, in turn, was obtained by a spectral expansion in terms of eigenfrequencies and eigenvectors of the Sturm–Liouville equation describing SH wave motion in the system adopting a slab approximation (for a short review, see Ref. 9).

(ii) We analyze the fluctuating polarization vector field P_y produced by the elasto-optic coupling when SH phonons modulate the dielectric function of the medium. The computation of the p-s Brillouin cross section is described in some detail. For this we use an electromagnetic Green function introduced some years ago by Laks and Mills[10] to solve an analogous problem in a quite different context.

(iii) Experimental spectra for SOI SIMOX structures are presented and compared to the theoretical calculations.

II. THE LAYER PROJECTED SPECTRAL DENSITY OF SH PHONONS

We assume that the free surface coincides with the $z = 0$ plane and that the z axis points downwards in the medium. The first interface is at $z = d$ and the second interface is at $z = L + d$. For SH waves propagating along any direction parallel to the $y = 0$ plane (which is both the sagittal and the scattering plane in our experiments) the relevant displacement field component is then u_y. The SH surface waves propagate along the x direction. We consider only [100] and [110] propagation directions for which the sagittal motion is decoupled from the SH one. The wave equation for u_y, when the x axis is parallel to [100], is written as

$$\rho(z)\frac{\partial^2 u_y}{\partial t^2} = C_{44}(z)\frac{\partial^2 u_y}{\partial x^2} + \frac{\partial}{\partial z}\left[C_{44}(z)\frac{\partial u_y}{\partial z}\right] \quad (1)$$

where the functions $\rho(z)$ and $C_{44}(z)$ take within each layer the value of the mass density and C_{44} elastic constant of the corresponding material.

Since the system is translationally invariant in the x direction parallel to the surface, we introduce the $(\omega, q_{||})$ Fourier component of the u_y SH displacement field (the parallel wave vector is $\mathbf{q}_{||} = q_{||}\hat{\mathbf{e}}_x$) as

$$u_y(\omega, q_{||}; x, z, t) = Q(\omega, q_{||})\phi_y(\omega, q_{||}, z)\exp[i(q_{||}x - \omega t)]. \quad (2)$$

where $Q(\omega, q_{||})$ is the normal coordinate of the SH phonon $(\omega, q_{||})$. Introducing (2) in the wave equation (1) we obtain the self-adjoint Liouville equation[11]

$$\frac{d}{dz}\left[C_{44}(z)\frac{d\phi_y(\omega, q_{||}, z)}{dz}\right] + [\rho(z)\omega^2 - C_{44}(z)q_{||}^2]\phi_y(\omega, q_{||}, z) = 0. \quad (3)$$

The mode z profiles $\phi_y(\omega, q_{||}, z)$ are the real eigenfunctions of Eq. (3) corresponding to the real eigenvalues $\omega^2 = \omega^2(q_{||})$, the SH phonon eigenfrequencies. The $\phi_y(\omega, q_{||}, z)$'s play, in the continuum model adopted here, the same role as the polarization unit vectors in lattice dynamics. A similar Liouville equation is obtained for the $\langle 110\rangle$ case substituting $\frac{1}{2}[C_{11}(z) - C_{12}(z)]$ for $C_{44}(z)$ as the multiplying coefficient of $q_{||}^2$ in (3).

Using a slab approximation[9] to solve the above spectral problem we impose the normalization conditions[11]

$$\int_0^h \rho(z)\phi_y^2(\omega, q_{||}, z)\, dz = 1, \quad (4)$$

the slab thickness being $h \gg L + d$. Also we assume stress-free boundary conditions which are written in terms of the vanishing of the z derivatives of the mode profiles at both the slab outer surfaces

$$\left(\frac{d\phi_y(\omega, q_{||}, z)}{dz}\right)_{z=0} = \left(\frac{d\phi_y(\omega, q_{||}, z)}{dz}\right)_{z=h} = 0\,. \quad (5)$$

Together with (4) and (5) Eq. (3) constitutes a well posed singular (at least in the case of sharp interfaces) Sturm-Liouville eigenvalue problem.[12]

In principle the spectrum of SH long-wavelength acoustic phonons in a semi-infinite (when the slab thickness h goes to infinity) layered medium is the union of a discrete and a continuous part. The latter starts at the transverse threshold of the substrate $\omega_t = c_t q_{||}$, where c_t is the shear horizontal sound velocity of the substrate in the appropriate propagation direction. In fact, at fixed $q_{||}$, only for $\omega > \omega_t$ do the partial plane waves in the unbounded substrate have a real perpendicular wave vector $q_\perp = (\omega^2/c_t^2 - q_{||}^2)^{1/2}$, as it must be for a nondecaying bulk wave. Thus, strictly speaking, only the discrete eigenvalues correspond to true surface modes (bounded states or resonances). Yet also in the continuous spectrum (where the mode profiles are not decaying in the substrate, corresponding to SH bulk waves reflecting at the surface) one can find considerable structure of surface character (quasi-resonances or pseudo-surface modes).

The adoption of the slab approximation produces only a discrete spectrum but the (still infinite but now numerable) eigenfrequencies separate into two classes: a limited number of eigenvalues with $\omega < \omega_t$ still correspond to the Love waves while all the other eigenvalues tend to accumulate from above toward ω_t and build a quasicontinuous spectrum provided the slab is sufficiently thick. It is then possible to compute the density of phonon states and to simulate in this way the true continuous spectrum of a semi-infinite medium.

The more or less surface character of these collective excitations can be judged from inspection of the layer projected phonon density of states (LPPDS) for the SH polarization

$$g_{yy}(\omega, q_{||}|z, z') = \sum_\alpha \sqrt{\rho(z)\rho(z')}\phi_y(\omega_\alpha(q_{||}), q_{||}, z) \times \phi_y(\omega_\alpha(q_{||}), q_{||}, z')\delta[\omega - \omega_\alpha(q_{||})]. \quad (6)$$

computed for $z = z'$:

$$g_{yy}(\omega, q_{||}|z, z) = \sum_{\alpha} \rho(z)\phi_y^2(\omega_\alpha(q_{||}), q_{||}, z) \times\delta[\omega - \omega_\alpha(q_{||})]. \quad (7)$$

Although $g_{yy}(\omega, q_{||}|z, z')$ in the case of Brillouin light scattering is not directly related to the cross section (see Sec. IV), as it is instead in the case of, e.g., low-energy electron surface scattering,[9] this quantity is useful to look at the surface localization of the phonon modes.

Introducing the retarded and advanced Green functions of Eq. (3) $G_{yy}(\omega \mp i\epsilon, q_{||}; z, z')$ as the solutions of the non-homogeneous equation

$$\frac{d}{dz}\left[C_{44}(z)\frac{dG_{yy}}{dz}\right] + [\rho(z)(\omega \mp i\epsilon)^2 - C_{44}(z)q_{||}^2]G_{yy} = \delta(z - z') \quad (8)$$

with the same boundary conditions as for the ϕ_y, a smooth representation $\bar{g}_{yy}(\omega, q_{||}|z, z)$ of the LPPDS for SH phonons can be obtained as

$$\bar{g}_{yy}(\omega, q_{||}|z, z) = \frac{\rho(z)}{2\pi i}[G_{yy}(\omega - i\epsilon, q_{||}; z, z) - G_{yy}(\omega + i\epsilon, q_{||}; z, z)] . \quad (9)$$

Once a sufficiently high number of eigenfrequencies and eigenfunctions of Eq. (3) has been obtained numerically[7] the Green functions can be computed by means of the spectral expansion[11]

$$G_{yy}(\omega \mp i\epsilon, q_{||}; z, z) = \sum_{\alpha} \frac{\phi_y^2(\omega_\alpha(q_{||}), q_{||}, z)}{(\omega \mp i\epsilon)^2 - \omega_\alpha^2(q_{||})}. \quad (10)$$

III. ELECTROMAGNETIC WAVE EQUATIONS FOR THE INCIDENT AND SCATTERED FIELDS IN THE MEDIUM

Neglecting thermal fluctuations cubic solids (to which we limit our treatment) have isotropic dielectric properties. The perturbation caused by long-wavelength acoustic phonons can be accounted for by means of an istantaneous anisotropic susceptibility, a second-order tensor the components of which are linear functions of the fluctuating elastic strains. Because of dispersion a simple constitutive law relating the polarization vector $\mathbf{P}$ to the electric field can be written only for monochromatic components. We assume that the electric field impinging from the vacuum onto the outer surface of the structure is a monochromatic plane p wave $(E_x, 0, E_z)$ with circular frequency ω_0 and consider at first only the presence of one $(\omega(q_{||}), q_{||})$ SH phonon [see Eq. (2)]. Taking into account the linearity of Maxwell equations and the smallness of thermal elastic strains the electromagnetic problem can be solved by first order perturbation theory.[1]

At zeroth order (neglecting the fluctuating part of the susceptibility and thus the scattered field) the electric field $\mathbf{E}^{\omega_0}(x, z)$ transmitted in the medium can be conveniently computed in terms of the y component of the magnetic induction field $B_y^{\omega_0}(x, z) = e^{i(k_{||}x)}B(z)$, where $k_{||} = (2\pi/\lambda)\sin\theta_i = (\omega_0/c)\sin\theta_i$ is the component parallel to the surface of the wave vector of the incident wave.[13] $B(z)$ satisfies the ordinary differential equation

$$\frac{d}{dz}\left(\frac{1}{\epsilon(z)}\frac{dB}{dz}\right) + \left(\frac{\omega_0^2}{c^2} - \frac{k_{||}^2}{\epsilon(z)}\right)B = 0. \quad (11)$$

$\epsilon(z)$ is the z profile of the complex relative dielectric function of the structure at frequency ω_0. In the ideal case $\epsilon(z)$ has a finite jump at each interface where the continuity of $B(z)$ and $\epsilon^{-1}(z)(dB/dz)$ is imposed and keeps a constant value in each layer. In the vacuum $(z < 0)$ $B(z) = (E_0/c)(e^{i(k_\perp z)} - r_p e^{-i(k_\perp z)})$, where E_0 is the electric field amplitude of the incident p wave, $k_\perp = (\omega_0/c)\cos\theta_i$ the component perpendicular to the surface of the wave vector of the incident wave, and r_p the reflection coefficient. Because the substrate is absorbing we impose also the condition that all electromagnetic fields vanish for $z \to \infty$. Once $B(z)$ has been computed $E_x^{\omega_0}(x, z)$ and $E_z^{\omega_0}(x, z)$ can be obtained as[13]

$$E_x^{\omega_0} = -i\frac{c^2}{\omega_0\epsilon(z)}\frac{\partial B_y^{\omega_0}}{\partial z} = -i\frac{c^2}{\omega_0\epsilon(z)}\frac{dB}{dz}e^{i(k_{||}x)}, \quad (12)$$

$$E_z^{\omega_0} = i\frac{c^2}{\omega_0\epsilon(z)}\frac{\partial B_y^{\omega_0}}{\partial x} = -\frac{c^2 k_{||}}{\omega_0\epsilon(z)}B(z)e^{i(k_{||}x)}. \quad (13)$$

The time dependence of all zeroth-order fields has been omitted and is $e^{-i\omega_0 t}$. The physical real fields are obtained taking the real parts of the full expressions.

The fluctuating part of the polarization vector in the medium, at first order, is

$$P_i^{\omega_s} = \epsilon_0[\epsilon(z) - 1]E_i^{\omega_s} + \epsilon_0\delta\chi_{ij}[\omega_0| \pm \omega_\alpha(q_{||})]E_j^{\omega_0}. \quad (14)$$

In the above equation $\epsilon(z) - 1 = \chi(z)$ is the unperturbed isotropic susceptibility in the absence of phonons [because $\omega_\alpha(q_{||}) \ll \omega_0$ we assume that $\epsilon[z|\omega_0 \pm \omega_\alpha(q_{||})] \approx \epsilon(z|\omega_0) = \epsilon(z)$] and $\delta\chi_{ij}(\omega_0| \pm \omega_\alpha(q_{||}))$ is the anisotropic fluctuating part of the susceptibility due the excitation of a single SH $(\omega_\alpha(q_{||}), q_{||})$ phonon mode. The second term in the right-hand side (rhs) of Eq. (14) is responsible for the radiation of the Brillouin light, that is, of the scattered field $\mathbf{E}^{\omega_s}$ at frequencies $\omega_s = \omega_0 \pm \omega_\alpha(q_{||})$.

Taking explicitly into account the elasto-optic coupling one finds that the part of the fluctuating polarization vector radiating the scattered field has only one component $(P_y^{\omega_s})_R$ which can be written in terms of the fluctuating thermal elastic strains $u_{yx} = \frac{1}{2}[\partial u_y(\omega_\alpha, q_{||})/\partial x]$ and $u_{yz} = \frac{1}{2}[\partial u_y(\omega_\alpha, q_{||})/\partial z]$ as[7]

$$(P_y^{\omega_s})_R = \epsilon_0 k_{44}(z)[u_{yx}(\omega_\alpha, q_{||})E_x^{\omega_0} + u_{yz}(\omega_\alpha, q_{||})E_z^{\omega_0}] \quad (15)$$

for [100] and as

$$(P_y^{\omega_s})_R = \epsilon_0 \Big\{ \tfrac{1}{2}[k_{11}(z) - k_{12}(z)] u_{yx}(\omega_\alpha, q_{||}) E_x^{\omega_0} + k_{44}(z) u_{yz}(\omega_\alpha, q_{||}) E_z^{\omega_0} \Big\} \quad (16)$$

for [110], where the $k_{ij}(z)$ are the z profiles of the relevant elasto-optic coefficients. Thus Brillouin scattering of an incident p electromagnetic wave off a pure SH phonon produces a scattered s electromagnetic wave, that is, scattering rotates the polarization of 90°.

In order to write down the wave equation for the scattered electric field component $E_y^{\omega_s}$ in a way suitable to compute the p-s Brillouin cross section we write again $(P_y^{\omega_s})_R$ in the compact form (for the sake of simplicity we report only the complex anti-Stokes term for [100], radiating at the circular frequency $\omega_s = \omega_\circ + \omega_\alpha(q_{||})$, corresponding to the annihilation of preexisting phonons)

$$(P_y^{\omega_s})_R = Q(\omega_\alpha, q_{||}) \Pi_y(z|\omega_0, k_{||}; \omega_\alpha, q_{||}) e^{i(k_{||}+q_{||})x}, \quad (17)$$

where

$$\Pi_y(z|\omega_0, k_{||}; \omega_\alpha, q_{||}) = \frac{c^2 \epsilon_0 k_{44}(z)}{2\omega_0 \epsilon(z)} \left[q_{||} \phi_y(\omega_\alpha(q_{||}), q_{||}, z) \frac{dB}{dz} - k_{||} \frac{d\phi_y(\omega_\alpha(q_{||}), q_{||}, z)}{dz} B(z) \right] \quad (18)$$

are spectral weights depending on both the phonon mode profiles and the zeroth order incident electromagnetic field in the medium. At thermal equilibrium the thermal average of $Q(\omega_\alpha, q_{||})$ is zero and so is that of the scattered field amplitude; thus the statistical properties of the Brillouin light depend on the probability density of the random variable $Q(\omega_\alpha, q_{||})$ and on its time autocorrelation function (see below). An equation similar to (18) is obtained for [110] using (16).

In the absence of free charge $\operatorname{div} \mathbf{E}^{\omega_s} = -\epsilon_0^{-1} \operatorname{div} \mathbf{P}^{\omega_s}$. Using this result together with Eqs. (14) – (17) in the system of Maxwell equations one finds the inhomogeneous wave equation for the radiation of the scattered field component $E_y^{s\alpha}(x,z,t) = E_y^\alpha(z) e^{i(k_{||}^s x - \omega_s t)}$ in the medium ($z > 0$)

$$\frac{d^2 E_y^\alpha}{dz^2} + \left[\epsilon(z) \frac{\omega_s^2}{c^2} - k_{||}^{s\,2} \right] E_y^\alpha = -\frac{\omega_s^2}{\epsilon_0 c^2} Q(\omega_\alpha, q_{||}) \Pi_y(z|\omega_0, k_{||}; \omega_\alpha, q_{||}) , \quad (19)$$

where $k_{||}^s = k_{||} + q_{||}$, expressing the conservation of parallel wave vector in an anti-Stokes event. In the vacuum above the surface ($z < 0$) the scattered field component $E_y^\alpha(z)$ obeys the homogeneous wave equation obtained by equating to zero the rhs of Eq. (19) with $\epsilon(z) = 1$ and takes the simple plane wave form $E_y^\alpha(z) = E_y^\alpha(0^-) e^{ik_\perp^s z}$ where $k_\perp^{s\,2} = \omega_s^2/c^2 - k_{||}^{s\,2}$. In the far field approximation the total scattered field in the vacuum within an infinitesimal solid angle $d\Omega$ around the direction of $\mathbf{k}^s = \mathbf{k}_\perp^s + \mathbf{k}_{||}^s$ coincides with its plane wave (Fourier) component $(\omega_s, \mathbf{k}^s)$. Thus the problem is reduced to the determination of $E_y^\alpha(0^-) = E_y^\alpha(0^+) = E_y^\alpha(0)$. This can be accomplished by means of the Green function $D_{yy}(\omega_s, k_{||}^s | z, z')$ of the above electromagnetic problem. D_{yy} is defined as the function obeying the same equations as $E_y^\alpha(z)$ does but with the rhs of Eq. (18) substituted by a delta function $\delta(z - z')$. Once D_{yy} is known one immediately has

$$E_y^\alpha(0) = -\frac{\omega_s^2}{\epsilon_0 c^2} Q(\omega_\alpha, q_{||}) \int_0^\infty \Pi_y(z'|\omega_0, k_{||}; \omega_\alpha, q_{||}) \times D_{yy}(\omega_s, k_{||}^s | 0, z')\, dz'. \quad (20)$$

In practice, because the skin depth of the electromagnetic field is much shorter than the slab thickness h, the integration in Eq. (20) can be stopped just at h.

The electromagnetic Green function can be expressed in terms of a matrix $d_{ij}(\omega_s, \mathbf{k}_{||}^s | z, z')$ which depends on $\mathbf{k}_{||}^s$ only through its modulus.[14] It turns out that $D_{yy} = d_{yy}$ for [100] and $D_{yy} = (d_{xx} + d_{yy})/2$ for [110]. The needed Green-function matrix d_{ij} has been taken from Ref. 10 where explicit formulas are available. Although the physical problem treated therein by Laks and Mills is quite different (photon emission from tunnel junctions) the mathematics of the radiation problem is exactly the same as that faced in the present paper.

In a scattering experiment the scattering geometry fixes $q_{||}$. Thus to obtain the total fluctuating scattered field component $(\omega, \mathbf{k}^s)$ one has to sum up (19) over all α's, that is, to consider the contribution of all phonons having the same parallel wave vector. The differential scattering cross section is proportional, through the factor $S \cos\theta_s$ (S is the illuminated area of the sample surface and θ_s the angle between $\mathbf{k}^s$ and the outgoing surface normal), to the thermal average of the power spectrum of the total scattered field component, that is to the time Fourier transform of its time autocorrelation function. We write the approximate scattered far field within $d\Omega$ around the direction of $\mathbf{k}^s$ as

$$E_y^s(\mathbf{r}, t) = -\frac{\omega_s^2}{\epsilon_0 c^2} e^{i\mathbf{k}^s \cdot \mathbf{r}} \sum_\alpha A_\alpha Q(\omega_\alpha, q_{||}) \times e^{i[\omega_0 + \omega_\alpha(q_{||})]t} , \quad (21)$$

where

$$A_\alpha = \int_0^h \Pi_y(z'|\omega_0, k_{||}; \omega_\alpha, q_{||}) D_{yy}(\omega_s, k_{||}^s | 0, z')\, dz'. \quad (22)$$

Making use of the fact that the $Q(\omega_\alpha, q_{||})$'s are independent random variables with mean square values fixed by the thermal equilibrium conditions $\langle Q_\alpha^2 \rangle_{\text{th}} = k_B T / S \omega_\alpha^2(q_{||})$, one finds that the differential scattering cross section for anti-Stokes Brillouin scattering from SH phonons is proportional to

$$\frac{d^2\sigma}{d\Omega d\omega} \propto \cos\theta_s \sum_\alpha \frac{|A_\alpha|^2}{\omega_\alpha^2(q_{||})}\delta[\omega - \omega_0 + \omega_\alpha(q_{||})]. \quad (23)$$

The Stokes cross section is derived similarly.

IV. EXPERIMENTAL RESULTS AND DISCUSSION

Brillouin spectra were acquired in backscattering at room temperature using a 3+3 passes tandem interferometer.[15] Measurements were performed using incident p-polarized light from an argon ion laser oscillating in single longitudinal mode at $\lambda_0 = 514.5$ nm wavelength and collecting only s-polarized scattered light. The laser power onto the sample surface was 150 mW. Spectra were taken at different angles of incidence, from 20° to 70°, in order to have different wave-vector components parallel to the surface $q_{||}$. To compensate for the parasitic broadening caused by the finite collection aperture, a vertical slit ($\Delta\theta \approx \pm 2°$) was used in the collection. This had also the advantage of avoiding the splitting of Brillouin scattering peaks in the spectra caused by the interception of the backscattered photons by the mirror used to direct the incident light onto the sample. With this configuration the integration time was four hours per measurement.

A Brillouin p-s spectrum taken along [100] at $\theta = 40°$ is presented as the upper line in Fig. 1. Two peaks are clearly visible and can be identified as being due to scattering from SH acoustic modes by comparison with the theoretical cross section which is drawn as the lower line in the same figure. In the calculation we used the dielectric (ϵ), elastic (C_{ij}), and elasto-optic constants of bulk Si and SiO_2. The Si constants are $\epsilon = 18.5 + 0.52i$, $C_{11} = 166$ GPa, $C_{12} = 63.9$ GPa, $C_{44} = 79.6$ GPa, $K_{11} = 53.2$, $K_{12} = 25.0$, $K_{44} = 23.4$, $\rho = 2330\,\mathrm{kg\,m^{-3}}$. The SiO_2 constants are $\epsilon = 2.16$, $C_{11} = 78.5$ GPa, $C_{44} = 31.2$ GPa, $K_{11} = -0.55$, $K_{44} = 0.345$, $\rho = 2200\,\mathrm{kg\,m^{-3}}$.

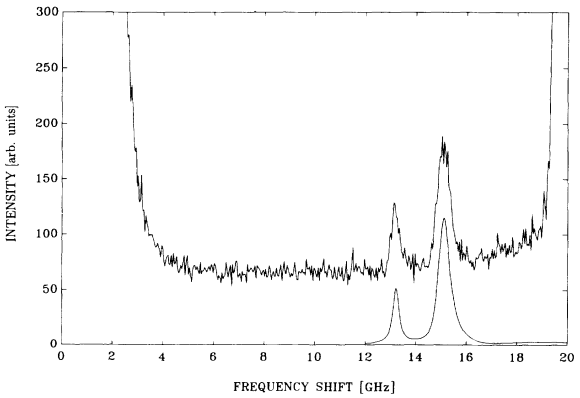

FIG. 1. Measured p-s Brillouin anti-Stokes spectrum (upper line) and theoretical p-s cross section (lower line) along ⟨100⟩ for $\theta = 40°$. The peak tail immediately at the right of zero shift belongs to the laser line while that growing near 20 GHz is due to an instrumental ghost of the interferometer.

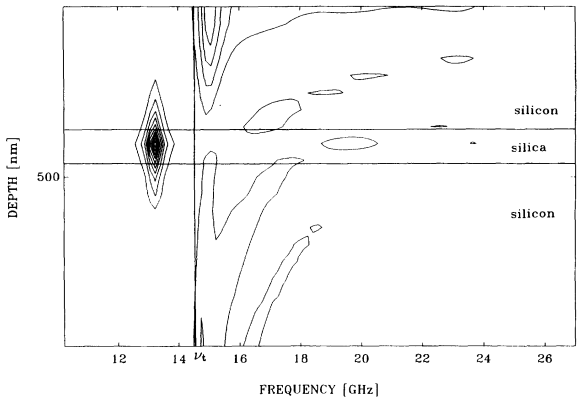

FIG. 2. Contour plot of the LPPDS as a function of depth and frequency calculated at 40° for propagation along ⟨100⟩. In the contour plot the geometry of the sample and the transverse threshold for silicon are evidenced. The first 300 eigenvalues and eigenfunctions of Eq. (3) were found using the NAG routine D02KEF based on a Prufer transformation and a shooting method. A total slab thickness h of 46 000 nm was taken. In Eq. (10) ϵ was taken equal to $2\pi \times 200$ Mrad s^{-1}.

The theory does not contain any free parameter but the theoretical cross section is convoluted with a Lorentzian of 200 MHz width to account for the finite experimental spectral resolution.

To explain the different acoustic nature of the peaks, in Fig. 2 a contour plot of $g_{yy}(\omega, q_{||}|z, z)$ is shown for a parallel wave vector $q_{||} \approx 0.0157\,\mathrm{nm^{-1}}$, corresponding to an incidence angle of $\theta_i = 40°$. The vertical line at $\nu_t = \omega_t/2\pi$ separates the discrete from the continuous spectrum. The mode below the threshold is highly localized within the silica buried layer (the transverse sound velocity of which is lower than that of silicon) and is a true surface wave decaying in the Si substrate (Love wave). The pronounced surface character of the pseudo-mode in the continuum above ν_t (pseudo-Love wave) is

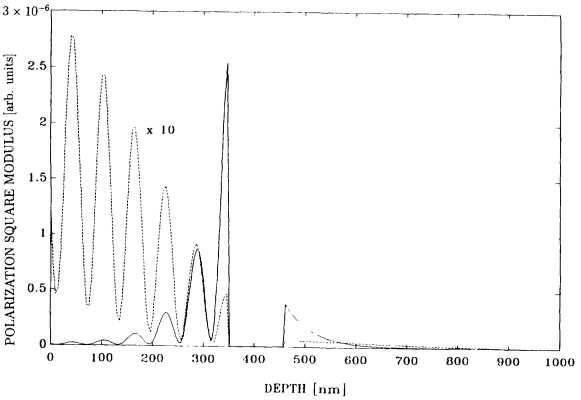

FIG. 3. Mean square polarization radiating the Brillouin light vs z at the frequency of the Love (full line) and of the pseudo-Love (dashed line) wave for $\theta_i = 40°$ and propagation direction [100]. It is seen that the source of the Brillouin light is confined in the Si layer immediately below the surface (see text).

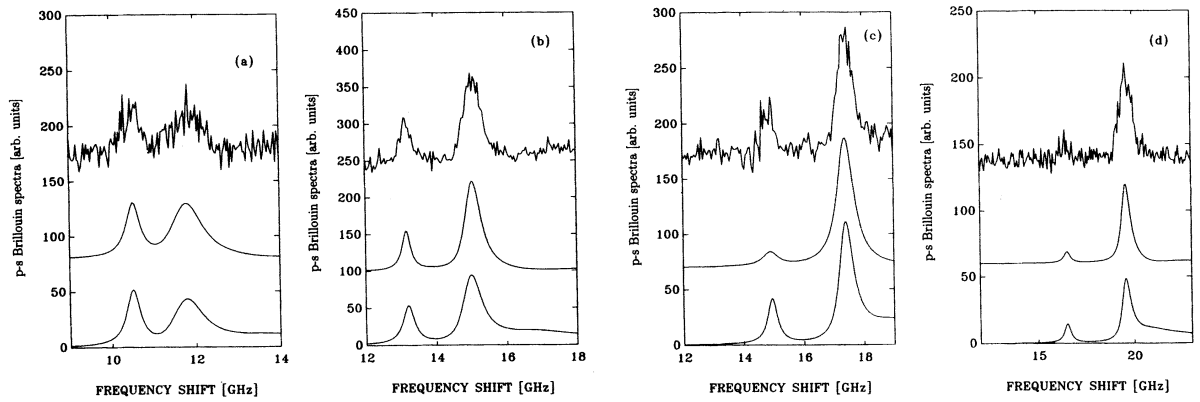

FIG. 4. From above: experimental p-s Brillouin spectra, theoretical cross section, and integral of LPPDS over the Si layer for four different backscattering geometries. (a) $\theta_i = 30°$; (b) $\theta_i = 40°$; (c) $\theta_i = 50°$; (d) $\theta_i = 60°$. Data have been normalized to the same area.

also visible.

The higher visibility of the pseudo–Love wave can be explained considering Fig. 3 where the mean square value of $(P_y^{\omega_s})_R$ vs z at $\theta_i = 40°$ is presented at two different frequencies: (a) that of the Love mode and (b) that of a mode in the continuum corresponding to the pseudo-Love peak. The source of Brillouin light [Eqs. (19)–(21)] is clearly confined in the Si layer $0 \leq z \leq d$. This is due to the fact that the k_{44} elasto-optic coefficient of Si is much larger than the corresponding quantity of silica (see above) and because the incident electric field transmitted in the medium is maximum there. The exponential vanishing of the source for $z \to \infty$ in the Si substrate is explained in terms of the vanishing of $B(z)$ due to absorption.

Although the Love wave is essentially a wave guided in the silica buried layer (see Fig. 2), only its upper tail contributes significantly to Brillouin scattering. The pseudo-Love wave has a high degree of localization in the silicon layer and is therefore highly visible.

In Fig. 4 the calculated p-s Brillouin differential cross sections [Eq. (23)] are compared to the experimental spectra at different incidence angles. The experimental spectra show an increase in the magnitude of the Love peak relatively to the pseudo-Love one for decreasing incidence angles in agreement with the theoretical cross-section predictions. The reason for this behavior is that the visibility of acoustic modes depends on their localization in the upper Si layer, as shown above.

An analysis of the LPPDS as a function of depth and frequency at several angles of incidence is useful in order to discuss the change in spatial localization for different $q_{||}$ (Fig. 5). In Fig. 5(a) we show the surface projected SH phonon density of states SPPDS= $g_{yy}(\omega, q_{||}|0,0)$ for four different values of θ_i (or $q_{||}$). It can be seen that the Love wave tends to become less confined in the silica layer for small $q_{||}$'s (its surface intensity increases) while the pseudo–Love wave has the highest surface intensity for $\theta_i \approx 40°$. In Fig. 5(b) $g_{yy}(\omega, q_{||}|z,z)$ is shown for $z =$ 400 nm about in the middle of the silica layer. Only the peaks corresponding to the Love wave are clearly visible. The enhancement of the peak amplitude as $q_{||}$ increases is evidence of the greater confinement of this mode in the silica layer. Since at small $q_{||}$ the Love wave is less confined in the silica and broadens in the Si layer [see Figs. 5(a) and 5(b)] its intensity increases. The pseudo-Love wave, the confinement of which in the Si layer does

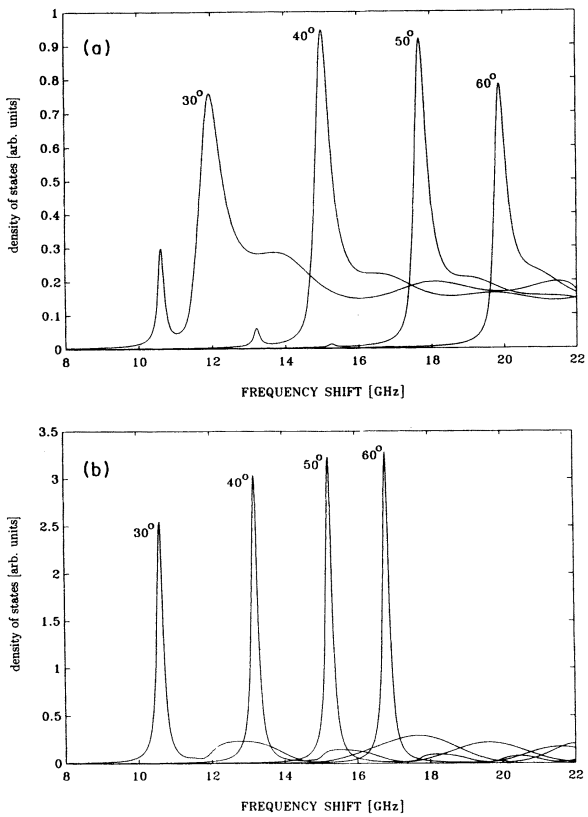

FIG. 5. Surface projected SH phonon density of states (a) and layer projected SH phonon density of states computed in the middle of the silica buried layer (b) for the same incident angles as in Fig. 4.

not depend strongly on $q_{||}$, always remains highly visible.

In Fig. 4 the lowest line (in each subplot) represents the thermal average of the integral of the LPPDS over the thickness d of the Si layer. The choice of this limit of integration is justified by the fact that only this region contributes to the intensity of the Brillouin light. It can be seen that this purely acoustic quantity is in reasonable agreement with the exact cross section. A qualitative explanation for this agreement goes as follows. The numerical computation shows that in Eq. 18, which gives the source for the radiation of the scattered field, the first term [proportional to the phonon displacement field $(\phi_y)_\alpha$] in the square brackets is dominant with respect to the second. Using in Eqs. (21) and (22) the fact that $D_{yy}(\omega_s, k^s_{||}|0, z')$ is a smooth function of z' for $0 \leq z' \leq d$ the coefficients A_α become simply proportional to the $(\phi_y)_\alpha$. Within this approximation the cross section becomes proportional to the thermal average of the integral of the SH LPPDS.

V. CONCLUSIONS

The computation of the cross section for Brillouin scattering of light by shear horizontal phonons for a medium consisting of a double layer on a substrate has been carried out. Brillouin scattering experiments have been performed on a silica layer buried in a Si(001) substrate using a backscattering geometry at different incidence angles and with an analysis of the s-polarized scattered light. Two peaks have been detected. The lower-frequency peak is the fingerprint of a shear horizontal mode (belonging to the discrete spectrum) which is confined in the silica layer (Love wave). The high-frequency peak has been identified as a quasiresonance in the continuous spectrum (pseudo-Love wave). The change in the visibility of both peaks as a function of the angle has been discussed. The relative intensity of the peaks is in good agreement with theoretical cross-section predictions.

ACKNOWLEDGMENTS

We gratefully aknowledge Dr. Laura Meda and Dr. G. F. Cerofolini of Istituto Donegani (Novara, Italy) for supply of the samples and S. Bertoni, of the same Institute, for electron microscopy. Many thanks are due to Professor F. Nizzoli for several discussions. A particular aknowledgement is due to Dr. P. Mutti for the initial suggestion of attempting Brillouin experiments on SOI SIMOX structures and to A. Mantegazza for technical advice. The presented activity was funded by Progetto Finalizzato Materiali Speciali per Tecnologie Avanzate of CNR.

---

* Also at Consorzio Interuniversitario di Fisica della Materia, Unità di Ricerca Milano Politecnico, Piazza Leonardo da Vinci, 32-20133 Milano, Italy

[1] V. Bortolani, F. Nizzoli, G. Santoro, and J. R. Sandercock, Phys. Rev. B **25**, 3442 (1982).

[2] P. Malischewsky, *Surface Waves and Discontinuities* (Elsevier, Amsterdam, 1987).

[3] V. Bortolani, A. M. Marvin, F. Nizzoli, and G. Santoro, J. Phys. C **16**, 1757 (1983).

[4] E. L. Albuquerque, R. Loudon, and D. R. Tilley, J. Phys. C **13**, 1775 (1980).

[5] A. P. Mayer, J. Phys. Condens. Matter **1**, 3957 (1989).

[6] J. A. Bell, R. Zanoni, C. T. Seaton, G. I. Stegeman, W. R. Bennett, and C. M. Falco, Appl. Phys. Lett. **52**, 610 (1988).

[7] C. E. Bottani, G. Ghislotti, and P. Mutti, J. Phys. Condens. Matter **6**, L85 (1994).

[8] F. Nizzoli, C. Byloos, L. Giovannini, C. E. Bottani, G. Ghislotti, and P. Mutti, Phys. Rev. B **50** 2027 (1994).

[9] D. L. Mills, S. Y. Tong, and J. E. Black, in *Surface Phonons*, edited by W. Kress and F. W. de Wette (Springer-Verlag, Berlin, 1991), p. 200.

[10] B. Laks and D. L. Mills, Phys. Rev. B **20**, 4962 (1979).

[11] R. Courant and D. Hilbert, *Methods of Mathematical Physics Vol. I* (Interscience Publisher, New York, 1953), p. 324

[12] H. Sagan, *Boundary and Eigenvalue Problems in Mathematical Physics* (Dover Publications, New York, 1989), p. 163

[13] J. Lekner, *Theory of Reflection* (Martinus Nijhoff Publishers, Dordrecht, 1987), pp. 5, 157.

[14] M. G. Cottam and A. A. Maradudin, in *Surface Excitations*, edited by V. M. Agranovich and R. Loudon (North-Holland, Amsterdam, 1984), p. 114.

[15] J. R. Sandercock, in *Light Scattering in Solids III*, edited by M. Cardona and G. Güntherodt, Topics in Applied Physics Vol. 51 (Springer-Verlag, Berlin, 1982), p. 173.